Inorg. Chem. **2003**, *42*, 7137–7147

Inorganic Chemistry
Article

Electrochemistry of Niobium(V) in Sulfuric and Methanesulfonic Acids: Formation of the $Nb_3O_2(SO_4)_6(H_2O)_3^{5-}$ Cluster and Designed Electrochemical Generation of "Nb_3O_2" Core Clusters by Double Potential Pulse Electrolysis

Michael May,[†] Melissa Gantt, Caroline Hoadley, Thomas Batten, William Sayers, and Vladimir Katovic*

Department of Chemistry, Wright State University, Dayton, Ohio 45435

Received April 30, 2003

The electrochemical and spectroelectrochemical properties of niobium(V) and the $Nb_3O_2(SO_4)_6(H_2O)_3^{5-}$ cluster in sulfuric acid and methanesulfonic acid were investigated using cyclic voltammetry, constant potential electrolysis, and spectroelectrochemistry. These chemical systems were suitable to probe the formation of "Nb_3O_2" core trinuclear clusters. In 9 M H_2SO_4 the cluster $Nb_3O_2(SO_4)_6(H_2O)_3^{5-}$ exhibited a reversible 1-electron reduction peak at $E_{pc} = -1.30$ V vs Hg/Hg_2SO_4 electrode, as well as a 4-electron irreversible oxidation peak at $E_{pa} = -0.45$ V. Controlled potential reduction at $E = -1.40$ V produced the green Nb(3.33+) cluster anion $Nb_3O_2(SO_4)_6(H_2O)_3^{6-}$. In 12 M H_2SO_4 Nb(V) displayed two reduction peaks at $E_{pc} = -1.15$ V and $E_{pc} = -1.30$ V. It was determined that the first process involves a quasi-reversible 2-electron reduction. After reduction of Nb(V) to Nb(III) the following chemical step involves formation of $[Nb(III)]_2$ dimer, which further reacts with Nb(V) to produce the $Nb_3O_2(SO_4)_6(H_2O)_3^{5-}$ cluster (ECC process). The second reduction peak at $E_{pc} = -1.30$ V corresponds to further 2-electron reduction of Nb(III) to Nb(I). The electrogenerated Nb(I) species also chemically reacts with starting material Nb(V) to produce additional $[Nb(III)]_2$. In 5 M H_2SO_4, the rate of the second chemical step in the ECC process is relatively slower and reduction of Nb(V) at $E = -1.45$ V/–1.2 V produces a mixture of $Nb_3O_2(SO_4)_6(H_2O)_3^{5-}$ and $[Nb(III)]_2$ dimer. $[Nb(III)]_2$ can be selectively oxidized by two 2-electron steps at $E = -0.65$ V to Nb(V). However, if the oxidation is performed at $E = -0.86$ V, the product is $Nb_3O_2(SO_4)_6(H_2O)_3^{5-}$. A double potential pulse electrolysis waveform was developed to direct the reduction of Nb(V) toward selective formation of the $Nb_3O_2(SO_4)_6(H_2O)_3^{5-}$ cluster. Proper application of dc-voltage pulses alternating between $E_1 = -1.45$ V and $E_2 = -0.86$ V yields only the target trinuclear cluster. Analogous double potential pulse electrolysis of Nb(V) in methanesulfonic acid generates the "Nb_3O_2" core cluster $Nb_3O_2(CH_3SO_3)_6(H_2O)_3^{+}$.

Introduction

It is well established that early transition metal ions in lower oxidation states often form metal clusters. However, little is known about the mechanism of metal cluster formation and therefore there are few designed synthetic procedures that would yield a desired cluster. Indeed, many metal clusters were discovered by chance.[1] Common synthetic preparations of early transition metal clusters involve chemical or electrochemical reduction of metal halides in molten salts at elevated temperature.[2] Later, Cotton reported that the trinuclear cluster $[Nb_3Cl_{10}(PR_3)_3]^-$ can be generated from the $[Nb_2Cl_7(PR_3)_2]^-$ intermediate and proposed the formation of dinuclear metal intermediates en route to trinuclear clusters.[3] He proposed two pathways for the generation of trinuclear clusters; the first involves reaction of dimer with monomer, while the second involves reaction of two dimers to give trinuclear cluster and monomer.

It has been long recognized that Nb(V), when reduced in sulfuric acid, produces intensely colored solutions. As early as 1839, Wohler observed blue, green, or red solutions from

---

* Corresponding author. E-mail: vladimir.katovic@wright.edu.

[†] Present address: Quality Control Lab, Isotec division (Sigma-Aldrich), Miamisburg, OH 45342.

(1) Cotton, F. A. *Q. Rev., Chem. Soc.* **1966**, *20*, 389.

(2) Masse, R.; Simon, A. *Mater. Res. Bull.* **1981**, *16*, 1007.

(3) Cotton, F. A.; Shang, M. *Inorg. Chem.* **1993**, *32*, 969.

10.1021/ic030145h CCC: $25.00

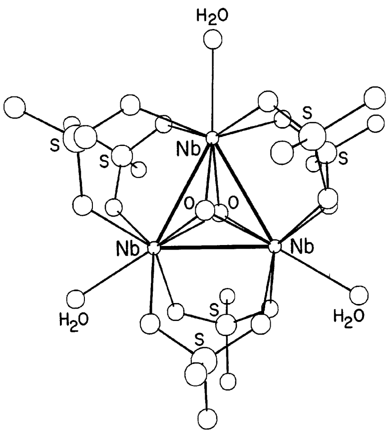

Figure 1. Structure of the $Nb_3O_2(SO_4)_6(H_2O)_3^{5-}$ anion.[12,13]

the acid reduction of Nb(V) with zinc depending upon sulfuric acid concentration.[4] Indeed, this characteristic color change was formerly used as a qualitative test for niobium. Subsequent work by Ott demonstrated that electrolysis of Nb(V) in sulfuric acid generated a red-brown solution from which stable potassium and ammonium salts were isolated.[5] There arose confusion in the early literature about the composition of such salts.[5,6] Following discovery of the metal−metal bonded hexanuclear cations $Mo_6Cl_8^{4+}$ and $Nb_6Cl_{12}^{2+}$,[7−9] formulas such as $K_8Nb_6O_3(SO_4)_{12}\cdot H_2O$ were proposed for the sulfate salts.[10,11] In 1980 Bino determined the crystal structure of a stable potassium salt and found its formula to be $K_4H_5O_2[Nb_3O_2(SO_4)_6(H_2O)_3]\cdot 5H_2O$.[12,13] The trinuclear cluster $Nb_3O_2(SO_4)_6(H_2O)_3^{5-}$ has been assigned to the M_3X_{17} structural type, with oxygen atoms below and above the Nb_3 triangle plane (see Figure 1). Two sulfate ligands bridge each side of the triangle, and three water molecules occupy equatorial positions. The formal oxidation state of niobium is 3.67+; thus four electrons occupy the metal bonding orbitals to give the Nb−Nb bond order 0.67. More recently, Richens and co-workers reported the preparation from Nb(III) precursor of trinuclear metal clusters having μ_3-Cl, μ_3-S, and μ_3-BO_3OH units.[14,15]

In prior work we reported that $Nb_3O_2(SO_4)_6(H_2O)_3^{5-}$ can electrocatalyze the reduction of H_2SO_4 to H_2S.[16] Here we extend such work to include the electrochemistry and spectroelectrochemistry of Nb(V) in sulfuric acid and methanesulfonic acid. These acid systems proved suitable to examine the formation of trinuclear clusters $Nb_3O_2(SO_4)_6(H_2O)_3^{5-}$ and $Nb_3O_2(SO_4)_6(H_2O)_3^{6-}$. In the course of this effort a pulse electrolysis waveform was designed to selectively drive Nb(V) reduction to $Nb_3O_2(SO_4)_6(H_2O)_3^{5-}$.

Experimental Section

Materials. $NbCl_5$ (99.1%), Nb_2O_5 (99.9%), H_2SO_4 (98%), and CH_3SO_3H (99.5%) were obtained from commercial sources and used as received. The trinuclear cluster salt $K_4H_5O_2[Nb_3O_2(SO_4)_6(H_2O)_3]\cdot 5H_2O$ was prepared by electrolytic reduction of Nb(V) in 12 M sulfuric acid at a mercury cathode according to Golibersuch and Young.[10]

Preparation of Nb(V) Solution in Sulfuric Acid. Nb_2O_5 (0.5 g) was fused with 5 g of $KHSO_4$ in a ceramic crucible. The melt was cooled and then dissolved in 20 mL of concentrated H_2SO_4. The solution was diluted with 20 mL of water, and niobium hydroxide was precipitated by addition of aqueous ammonia to pH 10 (**CAUTION!** exothermic reaction). The precipitate was separated by centrifugation and washed with aqueous ammonia until free of potassium cation (as determined by flame color test). It was dissolved in 18 M H_2SO_4, cooled, and carefully diluted to 12 M H_2SO_4.

This time-intensive procedure was improved by substituting $NbCl_5$ for Nb_2O_5. In a flask 2 g of $NbCl_5$ was hydrolyzed in 30 mL of water; upon gentle heating HCl gas evolved. The resultant solid was dissolved in 100 mL of 18 M H_2SO_4. After cooling, 25 mL of water was added, and the solution volume was adjusted to 350 mL by dilution with 12 M H_2SO_4 (**CAUTION**! exothermic reaction). This gave 0.02 M Nb(V) in 12 M sulfuric acid. Solutions of Nb(V) in 5 M H_2SO_4 were made from the latter solution by dilution with water cooled to 5 °C to avoid niobium hydroxide precipitation.

Preparation of Nb(V) Solution in Methanesulfonic Acid. About 0.75 g of $NbCl_5$ was hydrolyzed in water with heating. Several drops of aqueous ammonia were added to precipitate niobium hydroxide. After cooling, solid niobium hydroxide was isolated by centrifugation. The remaining solution was partially evaporated, and ammonia was again added to provide a second crop of niobium hydroxide. Fresh niobium hydroxide was then dissolved in methanesulfonic acid. Lastly water at 5 °C was added to constitute a 12 M solution.

Instrumentation. Constant potential electrolysis, coulometry, and cyclic voltammetry were performed with a PAR 173 potentiostat, PAR 175 programmer, PAR 179 digital coulometer, and xy-recorder. A hanging mercury-drop electrode (HMDE, PAR C9323) was utilized for cyclic voltammetry. Jacketed cells and a circulation bath were used to control solution temperature during experiments. Dc polarography was carried out using a PAR 174A potentiostat, dropping mercury electrode, Radiometer K601 Hg/Hg_2SO_4 reference electrode, and platinum auxiliary electrode. An H-geometry, jacketed electrolysis cell was equipped with quartz cuvette ($b = 2$ cm) and used for coulometry and spectroelectrochemistry (see Figure 2). This cell could be translated about the beam of a Varian 2300 UV−visible-IR spectrophotometer by a mechanical positioner. The latter device also incorporated a magnetic stirrer. Coulometry experiments utilized a mercury-pool working electrode.

Results and Discussion

Electrochemistry of $K_4H_5O_2[Nb_3O_2(SO_4)_6(H_2O)_3]\cdot 5H_2O$. When dissolved in 9 M sulfuric acid, $K_4H_5O_2[Nb_3O_2(SO_4)_6(H_2O)_3]\cdot 5H_2O$ yielded a red solution containing Nb_3O_2-

---

(4) Wohler, F. *Ann. Pogg.* **1839**, *48*, 93.
(5) Ott, F. *Z. Electrochem.* **1912**, *18*, 349.
(6) Kiehl, S. J.; Fox, R. L.; Hardt, H. B. *J. Am. Chem. Soc.* **1937**, *59*, 2395.
(7) Pauling, L. *Chem. Eng. News* **1947**, *25*, 2970.
(8) Vaughan, P. A.; Sturdivant, J. H.; Pauling, L. *J. Am. Chem. Soc.* **1950**, *72*, 5477.
(9) Brosset, C. *Ark. Kemi, Mineral. Geol.* **1945**, *A20* (7).
(10) Golibersuch, E. W.; Young, R. C. *J. Am. Chem. Soc.* **1949**, *71*, 2402.
(11) Krylov, E. I.; Kalugina, N. N. *Russ. J. Inorg. Chem. (Engl. Transl.)* **1959**, *4*, 1138.
(12) Bino, A. *J. Am. Chem. Soc.* **1980**, *102*, 7790.
(13) Bino, A. *Inorg. Chem.* **1982**, *21*, 1917.
(14) Minhas, S.; Richens, D. T. *J. Chem. Soc., Dalton Trans.* **1996**, 703.
(15) Minhas, S.; Devlin, A.; Richens, D. T.; Benyei, A. C.; Lightfoot, P. *J. Chem. Soc., Dalton Trans.* **1998**, 953.
(16) Paul, E. A.; Batten, T. H.; May, M. A.; Sayers, W. R.; Shelton, P. E.; Kojima, T.; Katovic, V. *Inorg. Chem.* **1994**, *33*, 630.

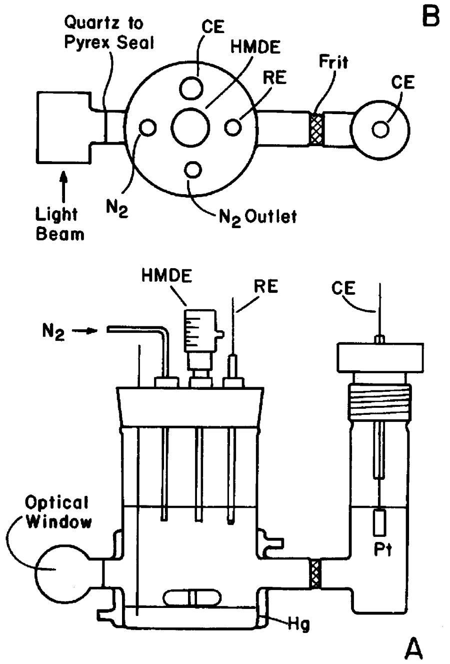

Figure 2. Schematic diagram of the electrolysis cell used for spectroelectrochemical studies: (A) front view; (B) top view.

$(SO_4)_6(H_2O)_3^{5-}$ anion, as concluded from absorption spectra obtained for the solid sample and solution.[12,13] The cyclic voltammogram of $K_4H_5O_2[Nb_3O_2(SO_4)_6(H_2O)_3]{\cdot}5H_2O$ in 9 M H_2SO_4 obtained at mercury drop electrode is shown in Figure 3A. The initial negative sweep displays a reduction peak at $E_{pc} = -1.3$ V vs Hg/Hg_2SO_4 electrode and a prominent oxidation peak at $E_{pa} = -0.45$ V. Based on criteria of cyclic voltammetry ($\Delta E_p = 58$ mV, $I_{pc}/I_{pa} = 1.0$), the reduction peak in Figure 3A corresponds to a 1-electron electrochemically reversible process.[17] The large oxidation peak at $E_{pa} = -0.45$ V is irreversible as shown by the absence of a coupled reduction current on the reverse scan. Constant potential electrolysis at $E = -1.4$ V changed the solution color from red to green, but due to proximity of the reduction potential to the solvent limit, the reduction current decayed only slowly to background level. The cyclic voltammogram obtained after exhaustive reduction at $E = -1.4$ V is shown in Figure 3B. It is similar to the voltammogram obtained before electrolysis, except that the peak near $E = -1.3$ V becomes anodic. Electrolytic reoxidation of this green solution at $E = -0.75$ V involved 0.97 mol of e^-/mol of Nb_3 cluster and changed the solution color back to red. The reversibility of this electrochemical redox couple is indicative of similar geometry for the two trinuclear anions. Thus the reduction peak at $E_{pc} = -1.3$ V involves reversible 1-electron reduction of the cluster:

$$Nb_3O_2(SO_4)_6(H_2O)_3^{5-} + e^- \rightarrow Nb_3O_2(SO_4)_6(H_2O)_3^{6-}$$

The formal oxidation state of niobium in $Nb_3O_2(SO_4)_6(H_2O)_3^{6-}$ is 3.33+; thus five electrons occupy the Nb_3 metal bonding orbitals.[18]

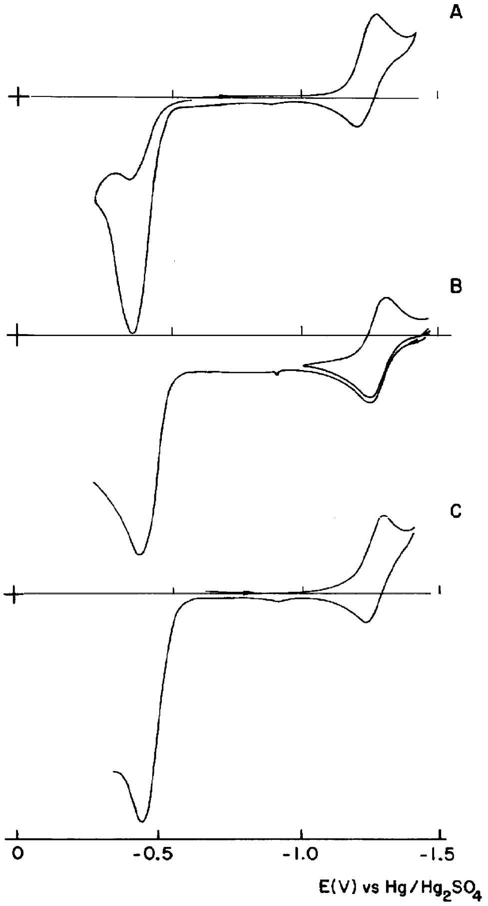

Figure 3. Cyclic voltammograms of 5×10^{-3} M $K_4H_5O_2[Nb_3O_2(SO_4)_6(H_2O)_3]{\cdot}5H_2O$ in 9 M H_2SO_4 using HMDE: (A) before electrolysis; (B) after electrolytic reduction at $E = -1.4$ V; (C) after successive reduction at $E_1 = -1.4$ V and reoxidation at $E_2 = -0.75$ V (scan rate = 50 mV/s).

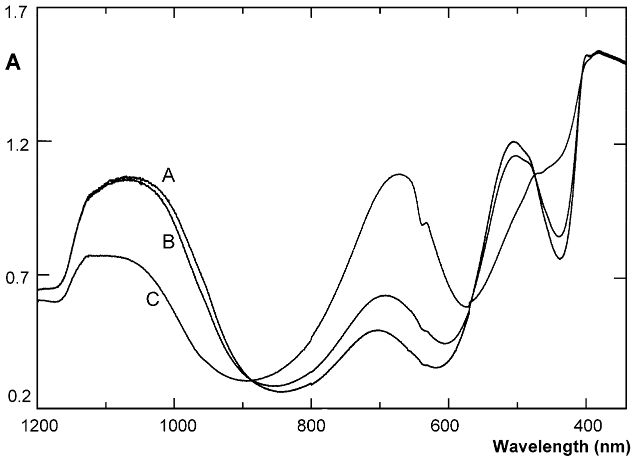

Figure 4. UV−visible spectra observed during the reduction of red $Nb_3O_2(SO_4)_6(H_2O)_3^{5-}$ solution (trace A) to green $Nb_3O_2(SO_4)_6(H_2O)_3^{6-}$ (trace C) at $E = -1.40$ V on Hg pool electrode. Trace B obtained after partial reduction.

An absorption spectrum of $Nb_3O_2(SO_4)_6(H_2O)_3^{5-}$ (see Figure 4A) consists of one broad band at 1065 nm and three bands at 703, 506, and 386 nm. The absorption spectrum of the electrogenerated $Nb_3O_2(SO_4)_6(H_2O)_3^{6-}$ cluster is shown in Figure 4B. It is interesting to note the spectral changes

---

[17] Bard, A. J.; Faulkner, L. R. *Electrochemical Methods*; John Wiley: New York, 1980.

[18] Cotton, F. A.; Duraj, S. A.; Roth, W. J. *J. Am. Chem. Soc.* **1984**, *106*, 3527.

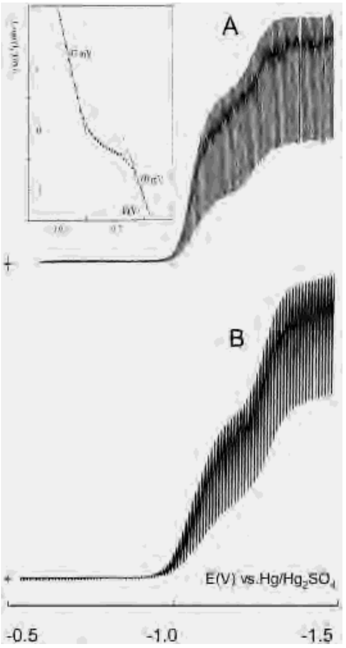

Figure 5. Dc polarograms of 2 × 10^{-2} M Nb(V) solution in 12 M H_2SO_4: (A) at +22 °C; (B) at −20 °C. The inset figure is a plot of $\log[(I_L - I)/I]$ vs $E_{applied}$ at +22 °C.

upon addition of one electron to the Nb_3 bonding orbital (compare Figure 4, trace A to B). Relative intensities of the 1065 and 506 nm bands decreased while the 703 nm peak increased in intensity and shifted in wavelength. Isosbestic points were observed near 890, 540, 480, and 410 nm, which indicate that only two species were involved in the reduction process. Electrolytic reoxidation of green $Nb_3O_2(SO_4)_6(H_2O)_3^{6-}$ at $E = -0.75$ V produced a red solution with an absorption spectrum characteristic of $Nb_3O_2(SO_4)_6(H_2O)_3^{5-}$. Controlled potential oxidation of $Nb_3O_2(SO_4)_6(H_2O)_3^{5-}$ at $E = -0.3$ V involved 3.9 mol of e^-/mol of Nb_3 and produced a colorless solution. The CV recorded in solution after the latter oxidation matches the voltammogram of Nb(V) in 9 M H_2SO_4 (see Figure 11A). Therefore the irreversible oxidation of $Nb_3O_2(SO_4)_6(H_2O)_3^{5-}$ at $E = -0.3$ V causes breakup of the trinuclear cluster and formation of Nb(V):

$$Nb_3O_2(SO_4)_6(H_2O)_3^{5-} + 4e^- \rightarrow 3Nb(V)$$

Electrochemistry of Nb(V) in 12 M H_2SO_4. The dc polarogram of Nb(V) in 12 M H_2SO_4 at +22 °C gave two well-defined reduction waves with half-wave potentials at $E_{1/2} = -1.07$ and -1.27 V vs Hg/Hg_2SO_4 (Figure 5A). Logarithmic analysis of the polarographic waves ($\log[(I_L - I)/I]$ vs $E_{applied}$) gave respective slopes of 47 and 60 mV. Since the slope of the first wave was less than the theoretical value of 58 mV, it probably involves a 2-electron, quasi-reversible process. This was also confirmed by coulometry (see Table 1). The slope of the second wave of 60 mV as well as its limiting current (half the first wave magnitude) indicates that it might involve a 1-electron reversible process. These results agree with previous polarography of Nb(V) in sulfuric acid.[19] However dc polarograms obtained at lower temperatures (Figure 5B) revealed that, as solution temperature was lowered, the relative height of the second wave increased and at −20 °C reached a magnitude comparable to that of the first wave. Similar behavior was also observed using CV (see Figure 8 later). On this basis it is proposed that the second wave also involves a 2-electron quasi-reversible process, that is, reduction of Nb(III) to Nb(I).

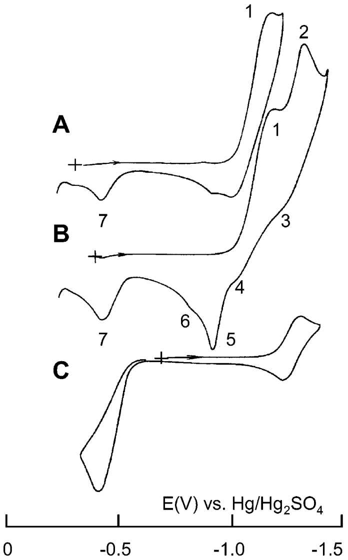

Figure 6. Cyclic voltammograms of 2 × 10^{-2} M Nb(V) solution in 12 M H_2SO_4 at +22 °C. The CV scan rate was 50 mV s^{-1}. (A) Potential reversed after the first reduction peak (peak 1). (B) Potential reversed after the second reduction peak (peak 2). (C) Cyclic voltammogram of $Nb_3O_2(SO_4)_6(H_2O)_3^{5-}$.

Table 1. Coulometric Data Obtained in 12 M H_2SO_4 at 0 °C

reaction	$E_{applied}$ (V)	$n_{apparent}$
$Nb(V) + 2e^- \rightarrow Nb(III)$	−1.22	1.34 mol of e^-/mol of Nb
$2Nb(III) + Nb(V) \rightarrow Nb_3O_2(SO_4)_6(H_2O)_3^{5-}$		
$Nb_3O_2(SO_4)_6(H_2O)_3^{5-} + e^- \rightarrow Nb_3O_2(SO_4)_6(H_2O)_3^{6-}$	−1.40	
$Nb_3O_2(SO_4)_6(H_2O)_3^{6-} \rightarrow Nb_3O_2(SO_4)_6(H_2O)_3^{5-} + e^-$	−0.75	0.97 mol of e^-/mol of Nb_3
$Nb_3O_2(SO_4)_6(H_2O)_3^{5-} \rightarrow 3Nb(V) + 4e^-$	−0.30	3.90 mol of e^-/mol of Nb_3

Cyclic voltammograms of 0.02 M Nb(V) solution in 12 M H_2SO_4 using HMDE are shown in Figure 6. For comparison Figure 6C also shows the cyclic voltammogram of $Nb_3O_2(SO_4)_6(H_2O)_3^{5-}$. On initial negative potential scan the cyclic voltammogram shown in Figure 6B gave two reduction peaks at $E_{pc} = -1.15$ V (peak 1) and $E_{pc} = -1.30$ V (peak 2). On the reverse positive potential scan, in addition to small coupled anodic peaks (peaks 3, 4) of the latter reductions, three new anodic peaks at $E_{pa} = -0.90$ V (peak 5), $E_{pa} = -0.82$ V (peak 6), and $E_{pa} = -0.45$ V (peak 7) were observed. Figure 6A is a cyclic voltammogram of Nb(V) obtained when the initial negative scan was reversed after the first reduction peak at $E = -1.25$ V, before the second reduction process could occur. This CV displays a reduction peak at $E_{pc} = -1.15$ V, its coupled anodic peak at $E_{pa} = -1.00$ V, a small oxidation peak at $E_{pa} = -0.90$ V, and another oxidation peak at $E_{pa} = -0.45$ V. Also, the

---

[19] Krylov, E. I.; Kolevateva, V. S.; Samarina, V. A. *Dokl. Akad. Nauk SSSR* **1954**, *98*, 593.

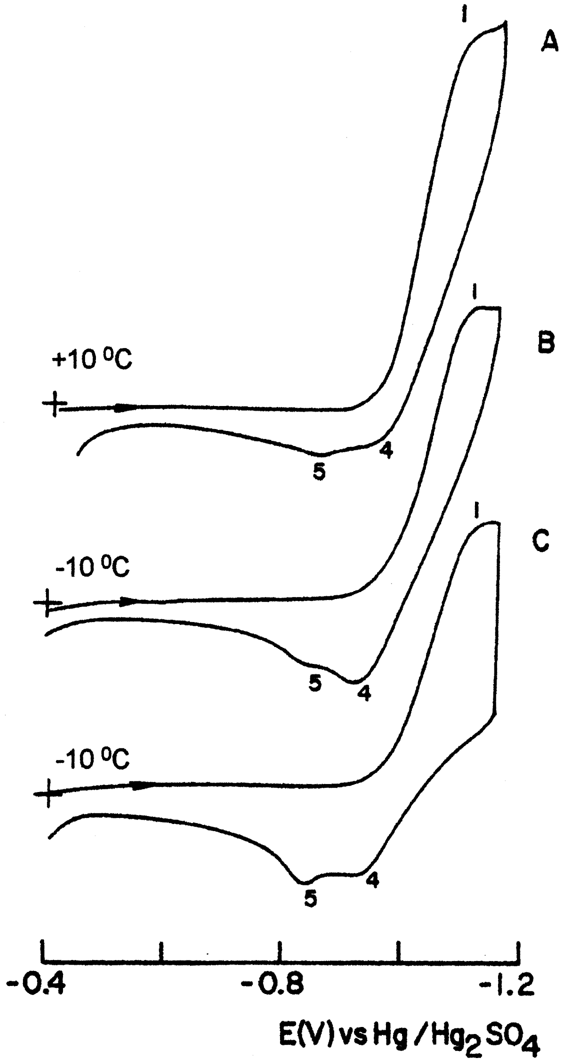

Figure 7. Cyclic voltammograms of 2×10^{-2} M Nb(V) solution in 12 M H_2SO_4 at +10 °C showing the first reduction peak only (trace A), −10 °C (trace B), and −10 °C coupled with a 30 s hold time at $E = -1.15$ V (trace C); scan rate = 50 mV/s.

oxidation processes (denoted peaks 5−7) were not observed if the potential was initiated at −1.0 V and first scanned in the positive direction. This implies that species at $E_{pa} = -0.90$, -0.82, and -0.45 V are formed by chemical steps that follow the initial electrochemical step.[17] For the first reduction process (peaks 1, 4) the peak potential separation $\Delta E_p = 160$ mV indicates quasi-reversible electron transfer, while the ratio of cathodic to anodic peak current $I_{pc}/I_{pa} \gg 1.0$ indicates that electron transfer is followed by chemical reactions. Temperature dependent cyclic voltammograms of peak 1 show that the electrogenerated reduction profile varies from +10 to −10 °C (see Figure 7). At +10 °C oxidation peak 4 (redox process Nb(III) − 2e$^-$ → Nb(V)) is small, indicating that Nb(III) is unstable. At lower temperature, −10 °C, the relative current for peak 4 increases, showing that its rate of chemical depletion is retarded. Trace C in Figure 7 was obtained at −10 °C with the applied potential held constant at $E = -1.15$ V for 30 s. In this case peak 5 becomes relatively larger than peak 4, indicating that the peak 5 species is generated from Nb(III).

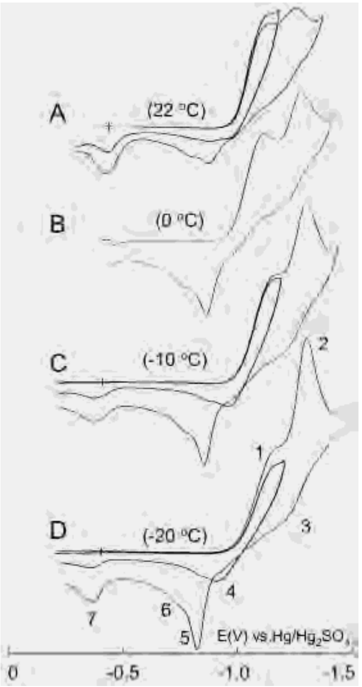

Figure 8. Cyclic voltammograms of 2×10^{-2} M Nb(V) solution in 12 M H_2SO_4 at (A) +22 °C; (B) 0 °C; (C) −10 °C; (D) −20 °C (scan rate = 50 mV/s).

Comparison of the cyclic voltammogram of Nb(V) in 12 M H_2SO_4 to that of $Nb_3O_2(SO_4)_6(H_2O)_3^{5-}$ (contrast Figure 6B to 6C) shows that CV peak 7 is due to the oxidation of $Nb_3O_2(SO_4)_6(H_2O)_3^{5-}$. This implies that the $Nb_3O_2(SO_4)_6(H_2O)_3^{5-}$ cluster is generated during the CV scan by chemical steps that rapidly follow an initial 2-electron reduction, and that oxidation peaks 5 and 6 arise due to the presence of an intermediate species. The second reduction peak at $E_{pc} = -1.4$ V is smaller than the first reduction peak when measured at room temperature. Following the same pattern obtained for dc polarograms, reduction peak 2 increased in size as temperature was lowered from +22 °C and achieved similar magnitude at −20 °C as the first peak. Figure 8 shows a series of Nb(V) cyclic voltammograms obtained from +22 to −20 °C. This behavior is consistent with the data obtained by dc polarography and confirms that the second reduction process also involves 2-electron reduction (Nb(III) + 2e$^-$ → Nb(I)).

An absence of coupled anodic current for peak 2 on the reverse scan, even at −20 °C, indicates that the reduction product, Nb(I), is also unstable and undergoes further chemistry. New anodic peaks at $E_{pa} = -0.90$ V (peak 5), $E_{pa} = -0.82$ V (peak 6), and $E_{pa} = -0.45$ V (peak 7) appear at the same potentials as they do in voltammograms when scan direction was reversed at $E = -1.25$ V. However, these peaks (denoted 5, 6, 7) are relatively larger in magnitude. Note the monotonic current increase for peak 2 and peak 5 as solution temperature was lowered. This indicates that at lower temperature the rate constant k_1 (see Scheme 1) decreased and more Nb(III) species is available for further reduction to Nb(I). Now the generated Nb(I) species is also not stable, and it undergoes further reaction to form additional Nb(III) intermediate. Thus it is proposed that electrochemi-

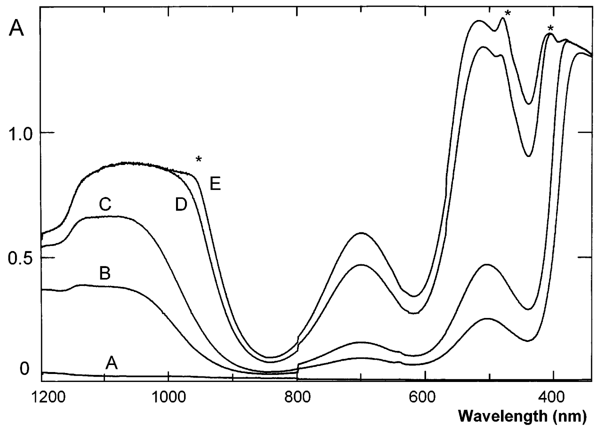

Figure 9. UV−visible spectral changes observed during electrolytic reduction in 12 M H_2SO_4 at $E = -1.22$ V vs Hg/Hg_2SO_4 electrode of colorless Nb(V) solution (trace A) to red $Nb_3O_2(SO_4)_6(H_2O)_3^{5-}$ (trace E).

Scheme 1

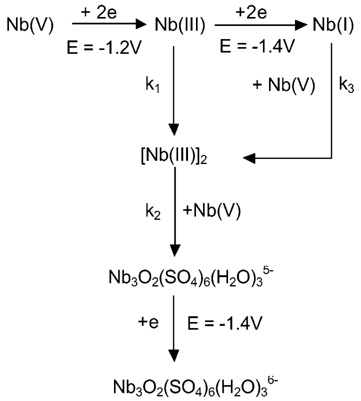

cally generated Nb(I) reacts with free Nb(V) to yield an additional amount of Nb(III) intermediate by a second reaction pathway (see Scheme 1). Based upon CV, dc polarography, spectroelectrochemistry, and coulometry (see Table 1), tentative peak assignments for the cyclic voltammogram of Nb(V) in 12 M H_2SO_4 are proposed:

peak 1:	$Nb(V) + 2e^- \rightarrow Nb(III)$	$E_{pc} = -1.15$ V
peak 2:	$Nb(III) + 2e^- \rightarrow Nb(I)$	$E_{pc} = -1.30$ V
peak 5:	oxidation of Nb(III) intermediate	$E_{pa} = -0.90$ V
peak 6:	oxidation of Nb(III) intermediate	$E_{pa} = -0.82$ V
peak 7:	$Nb_3O_2(SO_4)_6(H_2O)_3^{5-} \rightarrow 3Nb(V) + 4e^-$	$E_{pa} = -0.45$ V

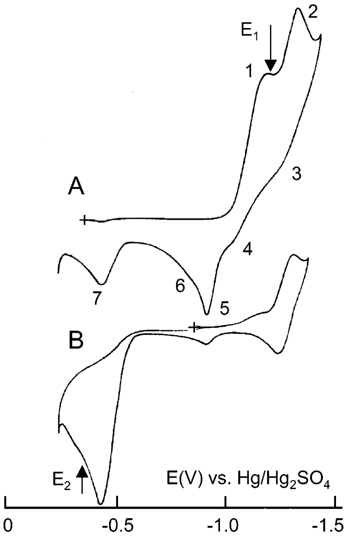

Figure 10. Cyclic voltammograms of Nb(V) in 12 M H_2SO_4 at 0 °C, at scan rate 50 mV s^{-1}: (A) before electrolysis; (B) after exhaustive electrolysis at $E = -1.22$ V.

Constant potential reduction of colorless Nb(V) solution at 0 °C, applied negative of the first reduction peak ($E_1 = -1.2$ V), consumed 1.34 mol of e^-/mol of Nb and produced a red solution. An absorption spectrum collected after partial electrolysis at $E_1 = -1.2$ V (see Figure 9, trace C) matched that of $K_4H_5O_2[Nb_3O_2(SO_4)_6(H_2O)_3]\cdot 5H_2O$, confirming that $Nb_3O_2(SO_4)_6(H_2O)_3^{5-}$ was electrochemically generated at this potential. The cyclic voltammograms of Nb(V) before and after electrolysis at $E_1 = -1.2$ V are shown in Figure 10. After electrolysis, peak 1, which is due to reduction of Nb(V) to Nb(III), almost completely disappeared and the oxidation peak at $E_{pa} = -0.45$ V became prominent. This anodic peak is also obtained if the potential scan is initiated at $E = -1.0$ V and first scanned in the positive direction. It is assigned to 4-electron oxidation of $Nb_3O_2(SO_4)_6(H_2O)_3^{5-}$ to Nb(V) since electrolytic reoxidation at $E_2 = -0.3$ V involved 1.3 mol of e^-/mol of Nb (3.9 mol of e^-/mol of Nb_3), and afterward gave a CV identical to that of Nb(V). The cyclic voltammogram in Figure 10B is similar to that of $Nb_3O_2(SO_4)_6(H_2O)_3^{5-}$; thus peaks 5 and 6 in Figure 10A correspond to the Nb(III) intermediate that is minor after the electrolysis, indicating that it is converted to $Nb_3O_2(SO_4)_6(H_2O)_3^{5-}$. We propose that the Nb(III) intermediate is $[Nb(III)]_2$ dimer, which reacts with the starting material Nb(V), to produce the $Nb_3O_2(SO_4)_6(H_2O)_3^{5-}$ cluster. Electronic spectra recorded during the constant potential reduction of Nb(V) on a mercury pool electrode in 12 M H_2SO_4 at 0 °C are shown in Figure 9 (trace A corresponds to pre-electrolysis Nb(V)). As the electrolysis at $E_1 = -1.2$ V proceeded, absorption bands at 386, 506, 703, and 1065 nm, which are characteristic of $Nb_3O_2(SO_4)_6(H_2O)_3^{5-}$, appeared and increased in intensity (see Figure 9, trace C). Toward the end of electrolysis, after approximately 1.2 mol of e^-/mol of Nb was consumed, two new absorptions at 964 and 463 nm appeared and increased in intensity (see trace E). However, these new bands were not observed in the UV−visible spectrum of $K_4H_5O_2[Nb_3O_2(SO_4)_6(H_2O)_3]\cdot 5H_2O$ in sulfuric acid. We propose that they arise from an intermediate $[Nb(III)]_2$ dimer that becomes stable only after the majority of Nb(V) is depleted. Thus the ECC reaction pathway at $E = -1.2$ V can be stated as

(E)	$Nb(V) + 2e^- \rightarrow Nb(III)$
(C)	$2Nb(III) \rightarrow [Nb(III)]_2$
(C)	$[Nb(III)]_2 + Nb(V) \rightarrow Nb_3O_2(SO_4)_6(H_2O)_3^{5-}$

Indeed, this proposed ECC sequence for Nb(V) fits a model developed by Bard in which reduction product **R** reacts with starting material **O** to yield product **P** (case IIb).[20] For the case of niobium in H_2SO_4 the reaction path first involves dimerization of reduction product **R**, followed by reaction of the dimer with starting material **O**:

---

[20] Geske, D. H.; Bard, A. J. *J. Phys. Chem.* **1959**, *63*, 1057.

$$\mathbf{O} + ne^- \rightarrow \mathbf{R} \qquad (k_h)$$
$$2\mathbf{R} \rightarrow \mathbf{R}_2 \qquad (k_1)$$
$$\mathbf{R}_2 + \mathbf{O} \rightarrow \mathbf{R}_2\mathbf{O} \qquad (k_2)$$

Bard's model predicts an apparent coulometric value of n_{app} that approaches "$2n/3$" when k_1 and k_2 are large, or a value of "n" when k_1 and k_2 approach zero. For intermediate values of k_2 and large values of k_1, or for low initial concentration of **O**, n_{app} can range between "2n/3" and "n" and the reduced solution would contain both $\mathbf{R}_2$ and $\mathbf{R}_2\mathbf{O}$. For the case of Nb(V) converted to $Nb_3O_2(SO_4)_6(H_2O)_3^{5-}$ the rate constants of the chemical steps are relatively large, as deduced from voltammetric data. The coulometric value of $n_{app} = 1.34$ mol of e$^-$/mol of Nb complements CV data. As theoretically predicted, the reduced solution can contain minor amounts of intermediate $\mathbf{R}_2$, if the initial concentration of species **O** is low or if k_2 is small. Our spectroscopic data show that near the start of electrolysis, when the concentration of Nb(V) was relatively high, the major product was $Nb_3O_2(SO_4)_6(H_2O)_3^{5-}$ and no $[Nb(III)]_2$ intermediate was observed. However, toward the end of electrolytic reduction, when the starting material Nb(V) is depleted, an intermediate species became observable; in addition to $Nb_3O_2(SO_4)_6(H_2O)_3^{5-}$ the electrolyzed solution also contained the intermediate, $[Nb(III)]_2$. Based upon the electrochemical data (CV and dcV), at lower temperatures it is proposed that a second reaction pathway operates to form $[Nb(III)]_2$ and ultimately $Nb_3O_2(SO_4)_6(H_2O)_3^{5-}$. The process involves reduction of Nb(III) to Nb(I), which is unstable in the presence of Nb(V) and also forms $[Nb(III)]_2$. The dimer reacts with starting material Nb(V) to form an additional amount of $Nb_3O_2(SO_4)_6(H_2O)_3^{5-}$. The extended scheme depicted in Scheme 1 is proposed for reduction of Nb(V) in 12 M sulfuric acid.

Electrochemistry of Nb(V) in 9 M and 5 M H_2SO_4. The cyclic voltammogram of Nb(V) in 9 M H_2SO_4 is similar to the voltammogram obtained in 12 M H_2SO_4, except that that the first reduction peak shifts negative and coalesces with the second reduction peak (see Figure 11A). Electrolysis in 9 M H_2SO_4 at $E = -1.4$ V first produced a red solution that upon prolonged electrolysis changed to green. Electronic spectra and voltammograms (see Figure 11) recorded at various stages of electrolysis show that after transfer of 1.33 mol of e$^-$/mol of Nb(V) the solution contains the $Nb_3O_2(SO_4)_6(H_2O)_3^{5-}$ cluster. Continued electrolysis at the same potential later produces a green solution containing $Nb_3O_2(SO_4)_6(H_2O)_3^{6-}$. Reoxidation of $Nb_3O_2(SO_4)_6(H_2O)_3^{6-}$ at $E = -1.1$ V, after consuming 0.33 mol of e$^-$/mol of Nb, gave a red solution containing $Nb_3O_2(SO_4)_6(H_2O)_3^{5-}$. Further oxidation of $Nb_3O_2(SO_4)_6(H_2O)_3^{5-}$ at $E = -0.40$ V involved 3.9 mol of e$^-$/mol of Nb_3 and caused breakup of the cluster to regenerate Nb(V).

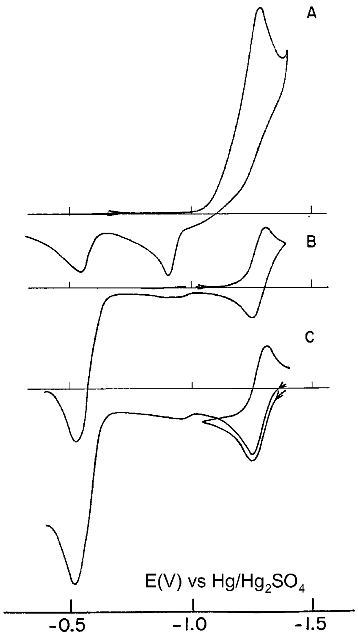

Figure 11. Cyclic voltammograms of 2×10^{-2} M Nb(V) solution in 9 M H_2SO_4 obtained during constant potential electrolysis at $E = -1.40$ V: (A) before electrolysis; (B) after electrolytic reduction of 1.33 mol of e$^-$/mol of Nb (Nb(V) $\rightarrow Nb_3O_2(SO_4)_6(H_2O)_3^{5-}$); (C) after further electroreduction to $Nb_3O_2(SO_4)_6(H_2O)_3^{6-}$ (scan rate = 50 mV/s).

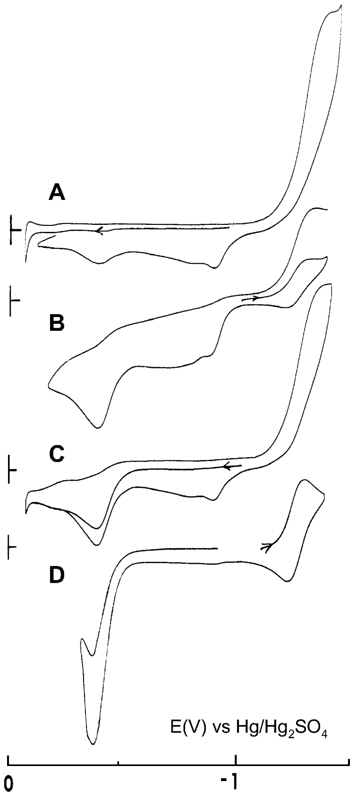

Figure 12. Series of cyclic voltammograms: (A) Nb(V) in 5 M H_2SO_4; (B) after reduction of Nb(V) at $E = -1.45$ V; (C) after successive electrolysis at $E_1 = -1.45$ V followed by $E_2 = -0.65$ V; (D) after successive electrolysis at $E_1 = -1.45$ V and $E_2 = -0.86$ V (applied potential vs Hg/Hg_2SO_4 reference electrode, scan rate = 50 mV/s).

A cyclic voltammogram of Nb(V) in 5 M H_2SO_4 (see Figure 12A) is similar to one obtained in 9 M H_2SO_4. It displays an irreversible multielectron reduction peak at $E_{pc} = -1.35$ V and three new oxidation peaks at $E_{pa} = -0.90$, -0.81, and -0.36 V upon reverse scan. The electrochemical behavior of Nb(V) in 5 M sulfuric acid is summarized in Scheme 2. Exhaustive reduction at $E = -1.45$ V, followed by reoxidation at $E = -1.2$ V, gave a red-brown solution (Scheme 2, step 1: note that electrolysis at $E = -1.45$ V generates $Nb_3O_2(SO_4)_6(H_2O)_3^{5-}$ that is further reduced to

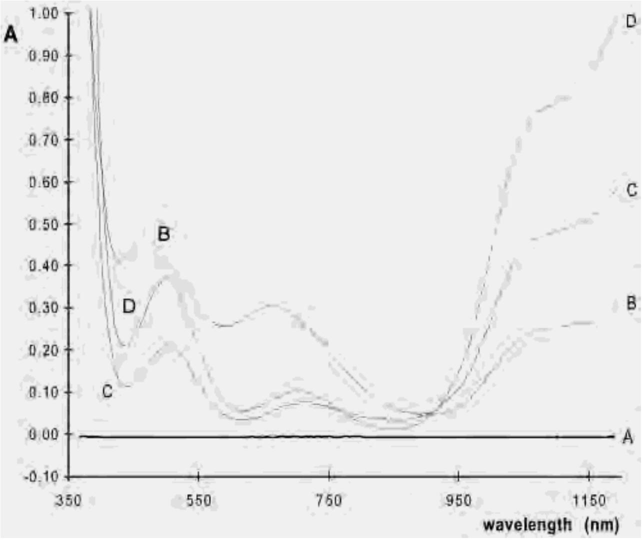

Figure 13. Series of Nb(V) UV−visible spectra in 5 M H_2SO_4 before electrolysis (trace A); following electrolytic reduction at $E = -1.45$ V (trace B); after successive electrolysis at $E_1 = -1.45$ V and $E_2 = -0.65$ V (trace C); after successive electrolysis at $E_1 = -1.45$ V and $E_2 = -0.86$ V (trace D).

Scheme 2

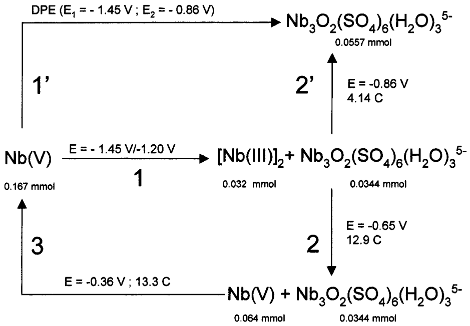

$Nb_3O_2(SO_4)_6(H_2O)_3^{6-}$; electrolytic oxidation at $E = -1.2$ V converts the latter to $Nb_3O_2(SO_4)_6(H_2O)_3^{5-}$). The cyclic voltammogram of this electrolyzed solution (see Figure 12B) confirms the presence of the $Nb_3O_2(SO_4)_6(H_2O)_3^{5-}$ cluster (irreversible oxidation peak at $E_{pa} = -0.36$ V and reduction peak at $E_{pc} = -1.3$ V) as well as the $[Nb(III)]_2$ intermediate (oxidation peaks at $E_{pa} = -0.90$, -0.81 V). In comparison to electrolysis in 12 M and 9 M H_2SO_4 that produced only minor amounts of intermediate, electrolysis in 5 M H_2SO_4 produced significant amounts of intermediate, indicating that the reaction rate for the second chemical step in the ECC process is lower in 5 M H_2SO_4. The electronic spectrum of the electrolyzed solution at $E = -1.45$ V/$E = -1.2$ V is shown in Figure 13B. From this solution it was found that $[Nb(III)]_2$ intermediate could be selectively oxidized to Nb(V) by constant potential oxidation at $E = -0.65$ V (Scheme 2, step 2). After selective oxidation of $[Nb(III)]_2$ the resultant solution contains $Nb_3O_2(SO_4)_6(H_2O)_3^{5-}$ cluster and Nb(V) as confirmed by CV (see Figure 12C) and its electronic spectrum (Figure 13C).

The relative amount of $Nb_3O_2(SO_4)_6(H_2O)_3^{5-}$ and $[Nb(III)]_2$ in the reduced solution at $E = -1.4$ V (step 1) was elucidated from coulometry, spectroscopy, and the initial amount of Nb(V). Selective reoxidation of the $[Nb(III)]_2$ intermediate to Nb(V) at $E = -0.65$ V consumed 12.9 C (step 2), while successive oxidation of $Nb_3O_2(SO_4)_6(H_2O)_3^{5-}$ to Nb(V) at $E = -0.36$ V consumed an additional 13.3 C (step 3). These 13.3 C correspond to the oxidation of 0.103 mmol of Nb(3.67+) equivalent to 0.0344 mmol of $Nb_3O_2(SO_4)_6(H_2O)_3^{5-}$. The same amount of $Nb_3O_2(SO_4)_6(H_2O)_3^{5-}$ cluster was obtained from absorbance measurements at 506 nm in Figure 13C. Subtracting 0.103 mmol of Nb(3.67+) from the initial amount of Nb(V) present before electrolysis (0.167 mmol of Nb) gives 0.064 mmol of Nb(III) (0.032 mmol of $[Nb(III)]_2$ dimer). The oxidation of 0.032 mmol of $[Nb(III)]_2$ at $E = -0.65$ V consumed 12.9 C; thus this process corresponds to 4-electron oxidation of $[Nb(III)]_2$ to two Nb(V). If the reduced solution containing a total of 0.167 mmol of niobium (as a mixture of 0.034 mmol of $Nb_3O_2(SO_4)_6(H_2O)_3^{5-}$ trimer and 0.032 mmol of $[Nb(III)]_2$ dimer) is reoxidized at a potential slightly positive of peak 5 ($E = -0.86$ V), the electrolysis product is exclusively $Nb_3O_2(SO_4)_6(H_2O)_3^{5-}$ cluster (Scheme 2, step 2′). Figure 12D shows the cyclic voltammogram obtained after successive electrolysis of Nb(V) in 5 M sulfuric acid at $E_1 = -1.45$ V and then at $E_2 = -0.86$ V. The voltammogram shows that the reoxidized product is exclusively $Nb_3O_2(SO_4)_6(H_2O)_3^{5-}$ cluster. Constant potential electrolysis at $E_2 = -0.86$ V consumed 4.14 C. This gives an n_{app} value of 0.6 mol of e^-/ mol of Nb(III). We propose the following reaction sequence in 5 M H_2SO_4 for electrochemical generation of the $Nb_3O_2(SO_4)_6(H_2O)_3^{5-}$ cluster by oxidation of $[Nb(III)]_2$ at $E_2 = -0.86$ V:

(E): $[Nb(III)]_2 - 2e^- \rightarrow [Nb(IV)]_2$
(C): $[Nb(IV)]_2 + [Nb(III)]_2 \rightarrow Nb_3O_2(SO_4)_6(H_2O)_3^{5-} + Nb(III)$

Corresponding spectroscopic data in 5 M H_2SO_4 support the premise that at $E_2 = -0.86$ V the dinuclear intermediate has been oxidized and the amount of $Nb_3O_2(SO_4)_6(H_2O)_3^{5-}$ formed increases relative to oxidation at $E_2 = -0.65$ V (see Figure 13C,D). By comparing peak absorbances at wavelength 506 nm in Figure 13, it is evident that there is a relative increase in the amount of $Nb_3O_2(SO_4)_6(H_2O)_3^{5-}$ if the second electrolysis is carried out at $E_2 = -0.86$ V. An effort to mathematically construct the UV−visible spectrum of the dinuclear intermediate is shown in Figure 14.

One highly practical outcome of this work was the development of a double potential, d.c.-pulse electrolysis waveform to drive reduction from Nb(V) directly to $Nb_3O_2(SO_4)_6(H_2O)_3^{5-}$. Selective formation of the latter cluster is accomplished by reducing Nb(V) in 5 M H_2SO_4 at $E_1 = -1.45$ V and then switching the potential to $E_2 = -0.86$ V which selectively oxidizes the intermediate to target product (Scheme 2, step 1′). By repetitive cycling of E_1/E_2 the metal cluster of interest, $Nb_3O_2(SO_4)_6(H_2O)_3^{5-}$, is selectively electrochemically generated. A cyclic voltammogram and electronic spectrum obtained after double potential pulse electrolysis in 5 M sulfuric acid was identical to the CV and spectra of $Nb_3O_2(SO_4)_6(H_2O)_3^{5-}$.

Electrochemistry of Nb(V) in 12 M Methanesulfonic Acid. It was of interest to examine the electrochemistry of

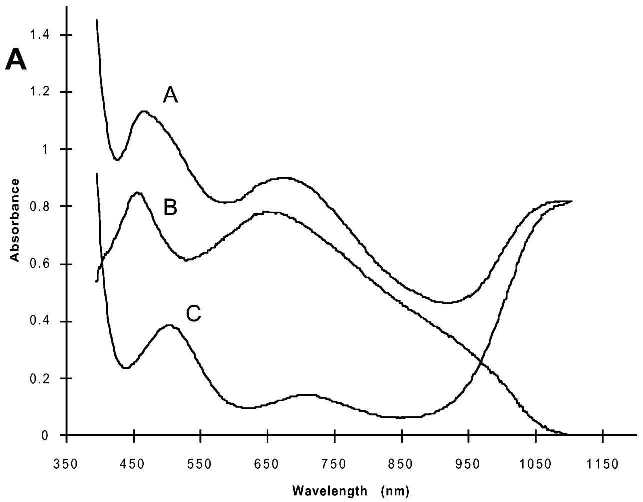

Figure 14. (A) UV−visible spectra of Nb(V) in 5 M H_2SO_4 following electrolytic reduction at $E = -1.45$ V vs Hg/Hg_2SO_4. (C) After successive electrolysis at $E_1 = -1.45$ V and $E_2 = -0.65$ V. (B) Difference spectrum of $[Nb(III)]_2$ dimer intermediate (trace A − trace C).

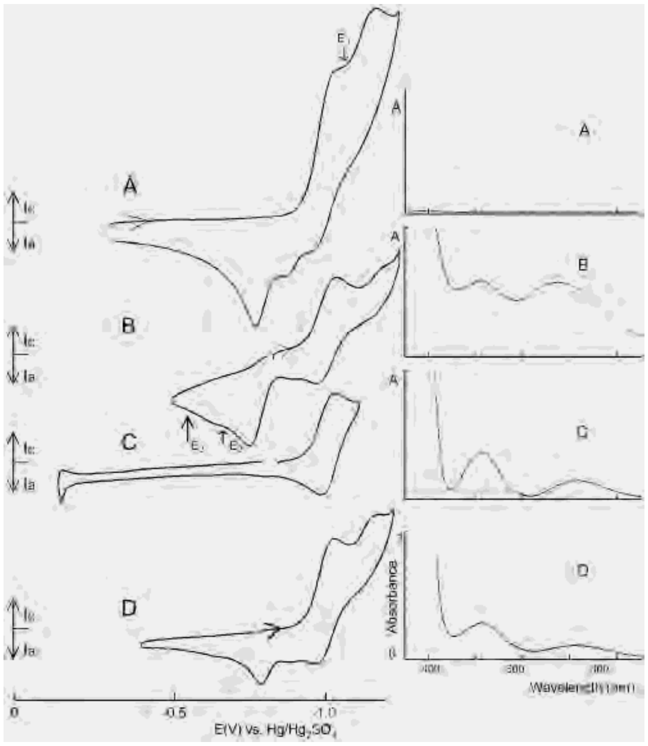

Figure 15. Cyclic voltammograms (left) and corresponding UV−visible spectra (right) of Nb(V) in 12 M CH_3SO_3H: (A) before electrolysis; (B) after electrolysis at $E_1 = -1.07$ V; (C) after successive electrolysis at $E_1 = -1.07$ and $E_2 = -0.67$ V; (D) after successive electrolysis at $E_1 = -1.07$ and $E_3 = -0.58$ V. Vertical arrows denote electrolysis potentials vs Hg/Hg_2SO_4.

Nb(V) in the methyl-substituted analogue of sulfuric acid since singly charged $CH_3SO_3^-$ anion would decrease the total negative charge on the cluster species from 5− to 1+, that is, $Nb_3O_2(CH_3SO_3)_6(H_2O)_3^+$ instead of $Nb_3O_2(SO_4)_6(H_2O)_3^{5-}$. A cyclic voltammogram of Nb(V) in 12 M methanesulfonic acid is shown in Figure 15A. The voltammogram is very similar to that obtained in 12 M H_2SO_4 (see Figure 6B), except that in CH_3SO_3H the peaks are shifted about 200 mV positive. As in 12 M H_2SO_4, the CV in CH_3SO_3H shows two reduction peaks at $E_{pc} = -1.00$ V and $E_{pc} = -1.12$ V. On reverse scan, the first reduction peak shows a small coupled oxidation peak at $E_{pa} = -0.9$ V indicating an EC process. Similarly, the second reduction peak does not show any anodic current on the reverse scan. However, a small oxidation peak at $E_{pa} = -0.8$ V is observed which probably corresponds to oxidation of an intermediate obtained by this EC process. As in 12 M H_2SO_4, a large anodic peak at $E_{pa} = -0.75$ V is observed indicating formation of intermediate, probably $[Nb(III)]_2$. By comparison to the CV in 12 M sulfuric acid, the voltammogram in 12 M methanesulfonic acid does not display a large anodic peak which would correspond to the oxidation of the trinuclear cluster. Probably any oxidation of the trinuclear cluster to Nb(V) is simply masked by mercury oxidation in CH_3SO_3H.

Constant potential electrolysis of Nb(V) in CH_3SO_3H is similar to the one obtained in 5 M H_2SO_4. Electrolysis of 0.33×10^{-3} mol of Nb(V) in 12 M CH_3SO_3H at a potential slightly negative of the first reduction peak ($E_1 = -1.07$ V) produced a red-blue solution. After transfer of 52 C, the solution gave the cyclic voltammogram shown in Figure 15B. It is visibly similar to the CV obtained in 5 M H_2SO_4 following reduction at $E = -1.45$ V. Cathodic peaks at $E_{pc} = -1.04$ and -1.12 V and anodic peaks at $E_{pa} = -0.95$ and -0.70 V were observed. The latter oxidation peaks are also observed if the CV is initiated at -0.8 V and first scanned in the positive direction. The cathodic peak at $E = -1.04$ V is about half the net height of the same peak before electrolysis at $E_1 = -1.07$ V and is better resolved. The second cathodic peak is nearly absent even though the applied potential was insufficient to reduce this species. UV−visible spectra obtained after electrolysis show two broad absorptions at 520 and 680 nm (Figure 15B).

Successive reoxidation of the electrolyzed solution in Figure 15B at $E_3 = -0.58$ V, slightly positive of the oxidation peak at $E_{pa} = -0.70$ V, consumed 13 C while the solution color changed to red. Following electrolysis, the absorption maximum at 680 nm decreased in intensity and shifted to 720 nm. The electronic spectrum obtained after reoxidation at $E_3 = -0.58$ V is almost identical to that of the $Nb_3O_2(SO_4)_6(H_2O)_3^{5-}$ cluster (compare Figure 15D to Figure 13D). By analogy to results from 5 M H_2SO_4, it is probable that electrochemical reduction of Nb(V) at $E_1 = -1.07$ V forms both $Nb_3O_2(CH_3SO_3)_6(H_2O)_3^+$ and $[Nb(III)]_2$ intermediate. For the case above, k_2 is presumably small and the reduced solution contains both trinuclear cluster and dimer.

In a separate set of experiments Nb(V) was reduced at $E_1 = -1.07$ V and reoxidized instead at $E_2 = -0.67$ V. The cyclic voltammogram and UV−visible spectrum of a solution obtained after reoxidation at $E_2 = -0.67$ V is shown in Figure 15C. Upon secondary electrolysis at $E_2 = -0.67$ V, the resultant UV−visible spectrum and CV indicate that only $Nb_3O_2(CH_3SO_3)_6(H_2O)_3^+$ anion is present in solution. Comparison of the spectrum obtained in solution after reoxidation at E_2 (Figure 15C) to one obtained after reoxidation at E_3 (Figure 15D) clearly shows that after oxidation at $E_2 = -0.67$ V an additional amount of cluster has been formed.

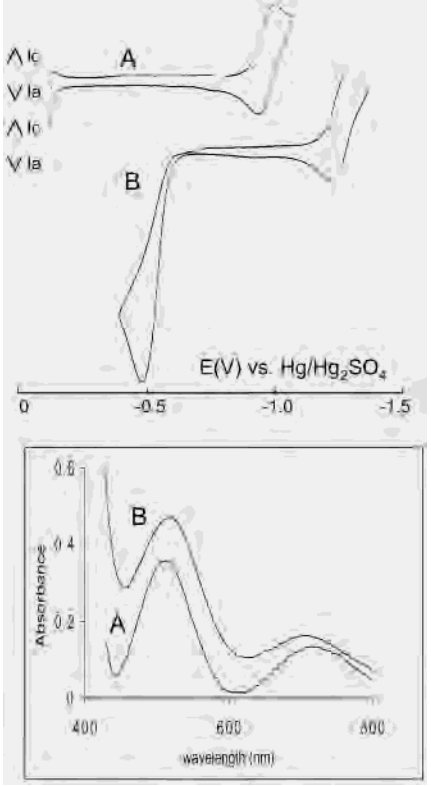

Figure 16. Cyclic voltammograms and corresponding UV−visible spectra: (A) Nb(V) in 12 M CH_3SO_3H after double potential pulse electrolysis at $E_1 = -1.07$ V and $E_2 = -0.67$ V; (B) $Nb_3O_2(SO_4)_6(H_2O)_3^{5-}$ in sulfuric acid solution (E vs Hg/Hg_2SO_4, scan rate = 50 mV/s).

This implies that trinuclear nobium cluster can be generated by two different reaction pathways:

$E_1 = -1.07$ V:
(E) $Nb(V) + 2e^- \rightarrow Nb(III)$
(C, k_1) $2Nb(III) \rightarrow [Nb(III)]_2$
(C, k_2) $[Nb(III)]_2 + Nb(V) \rightarrow Nb_3O_2(CH_3SO_3)_6(H_2O)_3^+$
$E_2 = -0.67$ V:
(E) $[Nb(III)]_2 - 2e^- \rightarrow [Nb(IV)]_2$
(C) $[Nb(IV)]_2 + [Nb(III)]_2 \rightarrow Nb_3O_2(CH_3SO_3)_6(H_2O)_3^+ + Nb(III)$

By applying pulsed electrolysis between $E_1 = -1.07$ V and E_2 -0.67 V, it was found that the Nb(V) reduction process could be driven to exclusively form the $Nb_3O_2(CH_3SO_3)_6(H_2O)_3^+$ cluster in a single step. Figure 16A shows the CV and the electronic spectrum obtained after double potential pulse electrolysis between E_1 and E_2. For comparison Figure 16B also shows the CV and electronic spectrum of the $Nb_3O_2(SO_4)_6(H_2O)_3^{5-}$ cluster anion. Their almost identical spectra and similar CV show that double potential step electrolysis of Nb(V) in CH_3SO_3H produces the analogous cluster $Nb_3O_2(CH_3SO_3)_6(H_2O)_3^+$.

Reaction Sequence for $Nb_3O_2(SO_4)_6(H_2O)_3^{5-}$. The chemical identity of Nb(V) species in 12 M H_2SO_4 is not known with certainty. It has been postulated that $NbO(SO_4)_2^-$ is the predominant species, since $NH_4NbO(SO_4)_2$ salt was isolated from H_2SO_4 solution.[21,22] The present dc-polarographic data indicate that one major electroactive species is present in 9−12 M sulfuric acid solution. Further, an earlier investigation of the Nb(V) polarographic wave in 12 M H_2SO_4 at $E_{1/2} = -1.07$ V reported the diffusion coefficient $D(Nb(V)) = 0.435 \times 10^{-5}$ cm^2 s^{-1}; the latter value is close to $D(Ti(IV)) = 0.550 \times 10^{-5}$ cm^2 s^{-1} under similar conditions, which is monomeric in 12 M H_2SO_4.[19] We believe that Nb(V) in 12 M sulfuric acid exists as $NbO(SO_4)_2^-$ since its ammonium salt was isolated as mentioned above.

The present electrochemical and spectroscopic data show that after 2-electron reduction of Nb(V) the resultant species, Nb(III), is not stable and forms an intermediate which reacts with starting material, Nb(V), to produce $Nb_3O_2(SO_4)_6(H_2O)_3^{5-}$. Further reduction of $Nb_3O_2(SO_4)_6(H_2O)_3^{5-}$ generates $Nb_3O_2(SO_4)_6(H_2O)_3^{6-}$, which was stable on the time scale of electrolysis. Assuming that Nb(V) in 12 M H_2SO_4 exists as $NbO(SO_4)_2^-$, the following ECC reaction sequence is tentatively proposed for electrochemical generation of cluster:

(E) $NbO(SO_4)_2^- + 2e^- + H^+ \rightarrow Nb(OH)(SO_4)_2^{2-}$
(C) $2Nb(OH)(SO_4)_2^{2-} \rightarrow Nb_2(OH)_2(SO_4)_4^{4-}$
(C) $Nb_2(OH)_2(SO_4)_4^{4-} + NbO(SO_4)_2^- + 2H_2O \rightarrow Nb_3O_2(SO_4)_6(H_2O)_3^{5-}$

We thus propose that the intermediate anion obtained from dimerization of Nb(III) is $Nb_2(OH)_2(SO_4)_4^{2-}$. Since the rate of the second chemical step in the ECC sequence above is lower in 5 M H_2SO_4, it implies that the detailed mechanism of trinuclear cluster formation likely involves protonation of $NbO(SO_4)_2^-$ following its coordination to the dinuclear intermediate. Similarly, the second pathway for formation of $Nb_3O_2(SO_4)_6(H_2O)_3^{5-}$ by two-electron oxidation of $[Nb(III)]_2$ at $E = -0.86$ V could be proposed as

(E) $Nb_2(OH)_2(SO_4)_4^{4-} - 2e^- \rightarrow Nb_2(OH)_2(SO_4)_4^{2-}$
(C) $Nb_2(OH)_2(SO_4)_4^{2-} + Nb_2(OH)_2(SO_4)_4^{4-} + 2H_2O \rightarrow Nb_3O_2(SO_4)_6(H_2O)_3^{5-} + Nb(OH)(SO_4)_2^{2-} + H^+$

It is possible that chemical pathways analogous to that above are operational in the formation of other electron-poor type trinuclear clusters. For instance, Cotton and co-workers found that a bioxo-capped, trinuclear molybdenum cation could be prepared by reaction of quadruply bonded molybdenum carboxylate dimer with MoO_4^{2-}:[23]

$$Mo_2(OCR)_4 + MoO_4^{2-} \rightarrow Mo_3O_2(OOCR)_6(H_2O)_3^{2+}$$

In 1993 Cotton presented several possible pathways for the formation of trinuclear metal clusters.[3] In one pathway, the trinuclear cluster could be formed by reaction of dimer with monomer. In another pathway two dimers react to form trinuclear cluster and monomer. For our case both of these pathways were observed in the formation of $Nb_3O_2(SO_4)_6(H_2O)_3^{5-}$ by electrochemical reduction. If the above proposed reaction sequences are correct, then it might be possible to prepare mixed-metal trinuclear clusters by designed pulse electrolysis. For example, from a solution with two different metal ions, the selective reduction of one

---

(21) Gohshtein, J. P. *Zh. Anal. Khim.* **1956**, *1*, 38.
(22) Goroschenko, J. G. *Zh. Neorg. Khim.* **1956**, *5*, 909.
(23) Cotton, F. A.; Dori, Z.; Marler, D. O.; Schwotzer, W. *Inorg. Chem.* **1983**, *22*, 3104.

metal species could produce MM dimer which further reacts with the second metal ion M′ to give mixed-metal cluster MMM′. One advantage of controlled pulse electrolysis is the capability to hold the concentration of select reactants high near the electrode, so that only the chemistry of interest proceeds.

IC030145H